



Queensland University of Technology
Brisbane Australia

This is the author's version of a work that was submitted/accepted for publication in the following source:

Frost, Ray L., López, Andrés, Belotti, Fernanda M., Xi, Yunfei, & Scholz, Ricardo
(2014)

A vibrational spectroscopic study of the phosphate mineral lulzacite $\text{Sr}_2\text{Fe}_{2+}(\text{Fe}_{2+}, \text{Mg})_2\text{Al}_4(\text{PO}_4)_4(\text{OH})_{10}$.

Spectrochimica Acta Part A: Molecular and Biomolecular Spectroscopy, 127, pp. 243-247.

This file was downloaded from: <https://eprints.qut.edu.au/69753/>

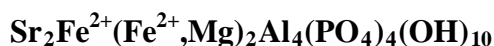
© Copyright 2014 Elsevier B.V.

NOTICE: this is the author's version of a work that was accepted for publication in *Spectrochimica Acta Part A*. Changes resulting from the publishing process, such as peer review, editing, corrections, structural formatting, and other quality control mechanisms may not be reflected in this document. Changes may have been made to this work since it was submitted for publication. A definitive version was subsequently published in *Spectrochimica Acta Part A*, [Volume 127, (5 June 2014)] DOI: 10.1016/j.saa.2014.02.041

Notice: *Changes introduced as a result of publishing processes such as copy-editing and formatting may not be reflected in this document. For a definitive version of this work, please refer to the published source:*

<https://doi.org/10.1016/j.saa.2014.02.041>

1 **A vibrational spectroscopic study of the phosphate mineral lulzacite**



3
4 **Ray L. Frost^{a*}, Andrés López,^a Fernanda M. Belotti^b, Yunfei Xi^a, Ricardo Scholz^c**

5
6 ^a School of Chemistry, Physics and Mechanical Engineering, Science and Engineering
7 Faculty, Queensland University of Technology, GPO Box 2434, Brisbane Queensland 4001,
8 Australia.

9
10 ^b Federal University of Itajubá, Campus Itabira, Itabira, MG, Brazil.

11
12 ^c Geology Department, School of Mines, Federal University of Ouro Preto, Campus Morro
13 do Cruzeiro, Ouro Preto, MG, 35,400-00, Brazil.

14
15 **Abstract:**

16 The mineral lulzacite from Saint-Aubin des Chateaux mine, France, with theoretical formula
17 $\text{Sr}_2\text{Fe}^{2+}(\text{Fe}^{2+},\text{Mg})_2\text{Al}_4(\text{PO}_4)_4(\text{OH})_{10}$ has been studied using a combination of electron
18 microscopy with EDX and vibrational spectroscopic techniques. Chemical analysis shows a
19 Sr, Fe, Al phosphate with minor amounts of Ga, Ba and Mg. Raman spectroscopy identifies
20 an intense band at 990 cm^{-1} with an additional band at 1011 cm^{-1} . These bands are attributed
21 to the PO_4^{3-} ν_1 symmetric stretching mode. The ν_3 antisymmetric stretching modes are
22 observed by a large number of Raman bands. The Raman bands at 1034, 1051, 1058, 1069
23 and 1084 together with the Raman bands at 1098, 1116, 1133, 1155 and 1174 cm^{-1} are
24 assigned to the ν_3 antisymmetric stretching vibrations of PO_4^{3-} and the HOPO_3^{2-} units. The
25 observation of these multiple Raman bands in the symmetric and antisymmetric stretching
26 region gives credence to the concept that both phosphate and hydrogen phosphate units exist
27 in the structure of lulzacite. The series of Raman bands at 567, 582, 601, 644, 661, 673 and
28 687 cm^{-1} are assigned to the PO_4^{3-} ν_2 bending modes. The series of Raman bands at 437,
29 468, 478, 491, 503 cm^{-1} are attributed to the PO_4^{3-} and HOPO_3^{2-} ν_4 bending modes.
30 No Raman bands of lulzacite which could be attributed to the hydroxyl stretching unit were
31 observed. Infrared bands at 3511 and 3359 cm^{-1} are ascribed to the OH stretching vibration
32 of the OH units. Very broad bands at 3022 and 3299 cm^{-1} are attributed to the OH stretching

* Author to whom correspondence should be addressed (r.frost@qut.edu.au)
P +61 7 3138 2407 F: +61 7 3138 1804

33 vibrations of water. Vibrational spectroscopy offers insights into the molecular structure of
34 the phosphate mineral lulzacite.

35

36 **Keywords:** lulzacite, strontium, phosphate, Raman spectroscopy

37

Introduction

The mineral lulzacite is a rare strontium containing phosphate mineral of general chemical formula $\text{Sr}_2\text{Fe}^{2+}(\text{Fe}^{2+},\text{Mg})_2\text{Al}_4(\text{PO}_4)_4(\text{OH})_{10}$. The mineral was first described in 2000 from quartzite deposits at Saint-Aubin-des-Châteaux, Loire-Atlantique, France [1]. The mineral occurs with quartz and siderite. Other minerals found with lulzacite include apatite, goyazite and pyrite [2]. Lulzacite is triclinic with *PI* space group, and unit cell parameters are: $a = 5.457(1) \text{ \AA}$, $b = 9.131(2) \text{ \AA}$, $c = 9.769(2) \text{ \AA}$, $\alpha = 108.47(3)^\circ$, $\beta = 91.72(3)^\circ$ and $\gamma = 97.44(3)^\circ$ [2]. The mineral is isostructural with jamesite ($\text{Pb}_2\text{Zn}(\text{Fe}^{2+},\text{Zn})_2\text{Fe}^{3+}_4(\text{AsO}_4)_4(\text{OH})_{10}$) [3, 4].

Raman spectroscopy has proven most useful for the study of mineral structure. Raman spectroscopy is an important tool in the characterization of phosphates in complex paragenesis [5-8]. In recent years, spectroscopic studies concerning phosphate minerals are increasing, especially due to their industrial and technological importance [8-11]. The aim of this paper is to report the Raman spectra of lulzacite, and to relate the spectra to the molecular structure of this hydrogen-phosphate mineral. The paper follows the systematic research of the large group of secondary minerals and especially molecular structure of minerals containing oxyanions using IR and Raman spectroscopy.

Experimental

Samples description and preparation

The lulzacite sample studied in this work forms part of the collection of the Geology Department of the Federal University of Ouro Preto, Minas Gerais, Brazil, with sample code SAC-106. The studied sample is from Saint-Aubin-des-Châteaux, located 8 km west of Châteaubriant (Loire-Atlantique, France). Quartzite forms a sequence of decimetric beds within Armorican sandstones. In the lower southwest part of the quarry, appears a micro-crystalline limestone level about 1 m thick, enriched in pyrite and organic matter. Veinlets filled mainly by quartz, siderite and recrystallised pyrite, with traces of sphalerite and galena, occur at the contact between quartzite and pyrite-rich limestone. Within these veinlets, phosphates are irregularly distributed and forms a complex paragenesis including lulzacite, goyazite, apatite and sulphides (pyrrhotite, pyrite, bournonite, boulangerite, sphalerite, galena and chalcopyrite) [2].

The sample was gently crushed and the associated minerals were removed under a stereomicroscope Leica MZ4. The lulzacite studied in this work occurs in association with

siderite. Scanning electron microscopy (SEM) in the EDS mode was applied to support the mineral characterization.

Scanning electron microscopy (SEM)

Experiments and analyses involving electron microscopy were performed in the Center of Microscopy of the Universidade Federal de Minas Gerais, Belo Horizonte, Minas Gerais, Brazil (<http://www.microscopia.ufmg.br>). Lulzacite massive fragment up to 0.5 mm was coated with a 5 nm layer of evaporated Au. Secondary Electron and Backscattering Electron images were obtained using a JEOL JSM-6360LV equipment. A qualitative and semi-quantitative chemical analysis in the EDS mode was performed with a ThermoNORAN spectrometer model Quest and was applied to support the mineral characterization.

Raman microprobe spectroscopy

Crystals of lulzacite were placed on a polished metal surface on the stage of an Olympus BHSM microscope, which is equipped with 10x, 20x, and 50x objectives. The microscope is part of a Renishaw 1000 Raman microscope system, which also includes a monochromator, a filter system and a CCD detector (1024 pixels). The Raman spectra were excited by a Spectra-Physics model 127 He-Ne laser producing highly polarized light at 633 nm and collected at a nominal resolution of 2 cm^{-1} and a precision of $\pm 1\text{ cm}^{-1}$ in the range between 200 and 4000 cm^{-1} . Repeated acquisitions on the crystals using the highest magnification (50x) were accumulated to improve the signal to noise ratio of the spectra. Raman Spectra were calibrated using the 520.5 cm^{-1} line of a silicon wafer. The Raman spectrum of at least 10 crystals was collected to ensure the consistency of the spectra.

An image of the lulzacite crystals measured is shown in the supplementary information as Figure S1. Clearly the crystals of lulzacite are readily observed, making the Raman spectroscopic measurements readily obtainable.

Infrared spectroscopy

Infrared spectra were obtained using a Nicolet Nexus 870 FTIR spectrometer with a smart endurance single bounce diamond ATR cell. Spectra over the $4000\text{--}525\text{ cm}^{-1}$ range were obtained by the co-addition of 128 scans with a resolution of 4 cm^{-1} and a mirror velocity of 0.6329 cm/s . Spectra were co-added to improve the signal to noise ratio.

Spectral manipulation such as baseline correction/adjustment and smoothing were performed using the Spectracalc software package GRAMS (Galactic Industries Corporation, NH, USA). Band component analysis was undertaken using the Jandel 'Peakfit' software package that enabled the type of fitting function to be selected and allows specific parameters to be fixed or varied accordingly. Band fitting was done using a Lorentzian-Gaussian cross-product function with the minimum number of component bands used for the fitting process. The Gaussian-Lorentzian ratio was maintained at values greater than 0.7 and fitting was undertaken until reproducible results were obtained with squared correlations of r^2 greater than 0.995.

Results and discussion

Chemical characterization

The BSE image of lulzacite sample studied in this work is shown in Figure 1. Qualitative and semi-quantitative chemical composition shows a Sr, Fe, Al phosphate with minor amounts of Ga, Ba and Mg. Carbon was observed due to effect of conductive tape and metallization.

The chemical analysis by EMP shows chemical formula expressed by $\text{Fe}^{2+}\text{Fe}_5^{3+}(\text{PO}_4)_4(\text{OH})_5 \cdot 4\text{H}_2\text{O}$ that indicate predominance of lulzacite member in a triple series between lulzacite, Zn-lulzacite and Al-lulzacite. Minor amount of Al was also found.

Vibrational Spectroscopy

Background

In aqueous systems, the Raman spectra of phosphate oxyanions show a symmetric stretching mode (ν_1) at 938 cm^{-1} , an antisymmetric stretching mode (ν_3) at 1017 cm^{-1} , a symmetric bending mode (ν_2) at 420 cm^{-1} and a ν_4 bending mode at 567 cm^{-1} . S.D. Ross in Farmer (page 404) listed some well-known minerals containing phosphate, which were either hydrated or hydroxylated or both [9]. The vibrational spectrum of the dihydrogen phosphate anion has been reported in Farmer. The PO_2 symmetric stretching mode occurs at 1072 cm^{-1} and the POH symmetric stretching mode at $\sim 878\text{ cm}^{-1}$. The position of the PO stretching vibration for calcium dihydrogen phosphate is found at 915 cm^{-1} . The POH antisymmetric stretching mode is at 947 cm^{-1} and the $\text{P}(\text{OH})_2$ bending mode at 380 cm^{-1} . The band at 1150

cm⁻¹ is assigned to the PO₂ antisymmetric stretching mode. The position of these bands will shift according to the crystal structure of archerite.

Raman and infrared Spectroscopy

The Raman spectrum of lulzacite over the 100 to 4000 cm⁻¹ spectral range is displayed in Figure 3a. This figure shows the position and relative intensities of the Raman bands. It may be observed that there are large parts of the spectrum where no Raman intensity is observed. Thus, the spectrum is subdivided into sections depending upon the type of vibration being examined. It is noted that significant intensity exists in the OH stretching region in the 2800 to 4000 cm⁻¹ spectral range, reflecting the number of hydroxyl units in the lulzacite structure. The infrared spectrum of lulzacite over the 500 to 4000 cm⁻¹ spectral range is shown in Figure 3b. This figure displays the position and relative intensity of the infrared bands. As for the Raman spectrum, the infrared spectrum is subdivided into sections based upon the type of vibration being studied.

The Raman spectrum of lulzacite over the 900 to 1200 cm⁻¹ spectral range is reported in Figure 4a. The spectrum is dominated by an intense Raman band at 990 cm⁻¹ which is attributed to the PO₄³⁻ ν₁ symmetric stretching vibrations. Two shoulder bands are found at 968 and 983 cm⁻¹. One possibility is that the proton of the hydroxyl unit is mobile and on a picoseconds time scale can transfer to the phosphate units, thus generating a HOPO₃²⁻ unit. A Raman band observed at 968 cm⁻¹ is attributed to the PO symmetric stretching vibration of these HOPO₃²⁻ units. A series of Raman bands of low intensity are noted at 1035, 1045, 1069, 1082, 1106 and 1128 cm⁻¹. These bands are assigned to the ν₃ antisymmetric stretching vibrations of PO₄³⁻ and the HOPO₃²⁻ units.

The infrared spectrum of lulzacite over the 650 to 1200 cm⁻¹ spectral range is shown in Figure 4b. This spectrum is complex and consists of a series of overlapping bands which may be curve resolved into component bands. The infrared bands at 972, 989 and 1007 cm⁻¹ may be assigned to the ν₁ symmetric stretching vibrations of PO₄³⁻ and the HOPO₃²⁻ units. The infrared bands at 1070, 1095, 1122 and 1153 cm⁻¹ are assigned to the ν₃ antisymmetric stretching vibrations of PO₄³⁻ and the HOPO₃²⁻ units.

The Raman spectrum of lulzacite over the 400 to 900 cm⁻¹ spectral range is given in Figure 5a. This figure shows the bands which are due to the bending modes of PO₄³⁻ and the

HOPO₃²⁻ units. The Raman bands at 412, 422 and 455 cm⁻¹ are assigned to the PO₄³⁻ and HOPO₃²⁻ ν_4 bending modes. The series of Raman bands at 506, 532, 579, 599, 615 and 627 cm⁻¹ are attributed to the PO₄³⁻ and HOPO₃²⁻ ν_2 bending modes.

A comparison may be based on that with other phosphate containing minerals, which also contain hydroxyl groups. For pseudomalachite Cu₅(PO₄)₂(OH)₄, Raman bands are observed at 482 and 452 cm⁻¹ of about equal intensity. The two ν_2 bands for pseudomalachite were reported by Ross [12] at 450 and 422 cm⁻¹. Cornetite Cu₃(PO₄)(OH)₃, Raman spectra shows an intense band at 433 cm⁻¹ with minor components at 463 and 411 cm⁻¹. Ross [9] reported two bands at 464 and 411 cm⁻¹ for cornetite. The variation between the spectral results may be attributed to orientation effects and the intensity of different bands will depend on which crystal face is scattering the Raman signal. The Raman spectrum of libethenite Cu₂(PO₄)(OH) showed a single band for ν_2 at 450 cm⁻¹. A number of bands in the 480 to 680 cm⁻¹ region of mineral phosphates were reported by Ross [12] for selected phosphates. Ross attributed these bands to the ν_4 modes. We observe similar number of bands for the churchite-(Y) minerals. The Raman spectrum of pseudomalachite exhibits bands at 481, 517, 537 and 609 cm⁻¹. The ν_4 modes for cornetite were observed at 487, 518, 541 and 570 cm⁻¹. Bands were observed for libethenite at 556, 582, 626 and 645 cm⁻¹. These band positions are in good agreement with the values reported by Ross in Farmer's treatise [12]. The Raman spectrum of the far low wavenumber region of lulzacite is shown in Figure 5b. A strong Raman band is noted at 227 cm⁻¹ which together with other bands in this spectral region are described as lattice vibrations. The Raman bands at 293, 326, 342, 365 and 393 are likely to be associated with metal oxygen stretching vibrations.

The Raman spectrum of lulzacite over the 3000 to 3700 cm⁻¹ spectral range is reported in Figure 6a. Two overlapping Raman bands at 3419 and 3447 cm⁻¹ together with the sharp intense Raman band at 3590 cm⁻¹ are assigned to the stretching vibrations of the OH units. The reason for the wide variation of the band position of the hydroxyl units is due to the variation in hydrogen bond strength of these hydroxyl units. The hydroxyl units are non-equivalent. Other low intensity shoulders are observed at 3345, 3554, 3605 and 3619 cm⁻¹. The low intensity Raman bands at 3105 and 3217 cm⁻¹ maybe due to the stretching vibrations of water. The infrared spectrum of lulzacite over the 2500 to 3800 cm⁻¹ spectral range is shown in Figure 6b. The intense infrared bands at 3420, 3596 and 3614 cm⁻¹ are assigned to the stretching vibration of OH units. The broader bands at 3070 and 3209 cm⁻¹ are attributed

to water stretching vibrations. The Raman spectrum of lulzacite over the 1400 to 1750 cm^{-1} is shown in Figure 7a. This spectrum suffers from a lack of signal. It is difficult to make a statement about Raman bands being present. The infrared spectrum of lulzacite over the 1300 to 1900 cm^{-1} spectral range is reported in Figure 7b. An infrared band is found at 1643 cm^{-1} which is ascribed to the bending vibration of strongly bonded water.

Conclusions

A lulzacite sample was studied by Electron Microscope in the EDS mode, Raman and infrared spectroscopy. The chemical analysis by EMP combined shows chemical formula expressed by $\text{Fe}^{2+}\text{Fe}_5^{3+}(\text{PO}_4)_4(\text{OH})_5 \cdot 4\text{H}_2\text{O}$ that indicate predominance of lulzacite member in a triple series between lulzacite, Zn-lulzacite and Al-lulzacite. Minor amount of Al was also found.

Raman spectroscopy identifies an intense band at 990 cm^{-1} and 1011 cm^{-1} . These bands are attributed to the PO_4^{3-} ν_1 symmetric stretching mode. The ν_3 antisymmetric stretching modes are observed by a large number of Raman bands. The Raman bands at 1034, 1051, 1058, 1069 and 1084 together with the Raman bands at 1098, 1116, 1133, 1155 and 1174 cm^{-1} are assigned to the ν_3 antisymmetric stretching vibrations of PO_4^{3-} and the HOPO_3^{2-} units. The observation of these multiple Raman bands in the symmetric and antisymmetric stretching region gives credence to the concept that both phosphate and hydrogen phosphate units exist in the structure of lulzacite. At least on the picoseconds time scale, the hydrogen phosphate units exist and may be identified by vibrational spectroscopy. The infrared spectrum shows complexity with many overlapping bands. The series of Raman bands at 567, 582, 601, 644, 661, 673 and 687 cm^{-1} are assigned to the PO_4^{3-} ν_2 bending modes. The series of Raman bands at 437, 468, 478, 491, 503 cm^{-1} are attributed to the PO_4^{3-} and HOPO_3^{2-} ν_4 bending modes. This work brings into question the actual formula of lulzacite $\text{Sr}_2\text{Fe}^{2+}(\text{Fe}^{2+}, \text{Mg})_2\text{Al}_4(\text{PO}_4)_4(\text{OH})_{10}$. The formula should include some hydrogen phosphate units.

Two overlapping Raman bands at 3419 and 3447 cm^{-1} together with the sharp intense Raman band at 3590 cm^{-1} are assigned to the stretching vibrations of the OH units. Infrared bands at 3511 and 3359 cm^{-1} are ascribed to the OH stretching vibration of the OH units. Very broad bands at 3022 and 3299 cm^{-1} are attributed to the OH stretching vibrations of water.

239 Vibrational spectroscopy offers insights into the molecular structure of the phosphate mineral
240 lulzacite.

241

242 **Acknowledgements**

243 The financial and infra-structure support of the Discipline of Nanotechnology and Molecular
244 Science, Science and Engineering Faculty of the Queensland University of Technology, is
245 gratefully acknowledged. The Australian Research Council (ARC) is thanked for funding the
246 instrumentation. The authors would like to acknowledge the Center of Microscopy at the
247 Universidade Federal de Minas Gerais (<http://www.microscopia.ufmg.br>) for providing the
248 equipment and technical support for experiments involving electron microscopy.

References

- [1] Y. Moelo, B. Lasnier, P. Palvadeau, P. Leone, F. Fontan, *Compt. Rend.* 330 (2000) 317-324.
- [2] P. Leone, P. Palvadeau, Y. Moelo, *Compt. Rend.* 3 (2000) 301-308.
- [3] Y. Moelo, O. Rouer, M. Bouhnik-Le Coz, *Euro. J. Min.* 20 (2008) 205-216.
- [4] P. Keller, H. Hess, P.J. Dunn, *Chem. Erde*, 40 (1981) 105-109.
- [5] M. Łodziński, M. Sitarz, *J. Mol. Struct.* 924-926 (2009) 442-447.
- [6] R.L. Frost, Y. Xi, R. Scholz, F.M. Belotti, M.C. Filho, *J. Mol. Struct.* 1033 (2013) 258-264.
- [7] R.L. Frost, R. Scholz, A. Lopes, Y. Xi, Z.Z. Gobac, L.F.C. Horta, *Spectrochim. Acta*, A116 (2013) 491-496.
- [8] R.L. Frost, A. Lopez, Y. Xi, A. Granja, R. Scholz, *Spectrochim. Acta*, A115 (2013) 22-25.
- [9] L.A.d.S. Costa, C. Souza de Miranda, M.I. Campos, D.d.J. Assis, J.I. Druzian, *Revista GEINTEC*, 3 (2013) 055-069.
- [10] J. Jimenez-Guzman, L. Gomez-Ruiz, M. Garcia-Garibay, *Informacion Tecnologica*, 14 (2003) 7-12.
- [11] K.C. Sekhar, C.T. Kamala, N.S. Chary, A.B. Mukherjee, *Trace Metals and Other Contaminants in the Environment*, 9 (2007) 315-337.
- [12] V.C. Farmer, *Mineralogical Society Monograph 4: The Infrared Spectra of Minerals*, published by The Mineralogical Society, London, 1974.

279
280
281
282
283
284
285
286
287
288
289
290
291
292
293

294 **List of figures**

295

296 **Figure 1 - Backscattered electron image (BSI) of a lulzacite crystal fragment up to 0.5**
297 **mm in length.**

298

299 **Figure 2 - EDS analysis of lulzacite**

300

301 **Figure 4 (a) Raman spectrum of lulzacite over the 4000 to 100 cm⁻¹ spectral range (b)**
302 **Infrared spectrum of lulzacite over the 4000 to 500 cm⁻¹ spectral range**

303

304 **Figure 5 (a) Raman spectrum of lulzacite over the 1400 to 800 cm⁻¹ spectral range (b)**
305 **Infrared spectrum of lulzacite over the 1300 to 500 cm⁻¹ spectral range**

306

307 **Figure 6 (a) Raman spectrum of lulzacite over the 800 to 300 cm⁻¹ spectral range (b)**
308 **Raman spectrum of lulzacite over the 300 to 100 cm⁻¹ spectral range**

309

310 **Figure 7 (a) Raman spectrum of lulzacite over the 3800 to 2600 cm⁻¹ spectral range (b)**
311 **Infrared spectrum of lulzacite over the 3800 to 2600 cm⁻¹ spectral range**

312

313 **Figure 8 (a) Raman spectrum of lulzacite over the 1800 to 1400 cm⁻¹ spectral range (b)**
314 **Infrared spectrum of lulzacite over the 1800 to 1300 cm⁻¹ spectral range**

315

316

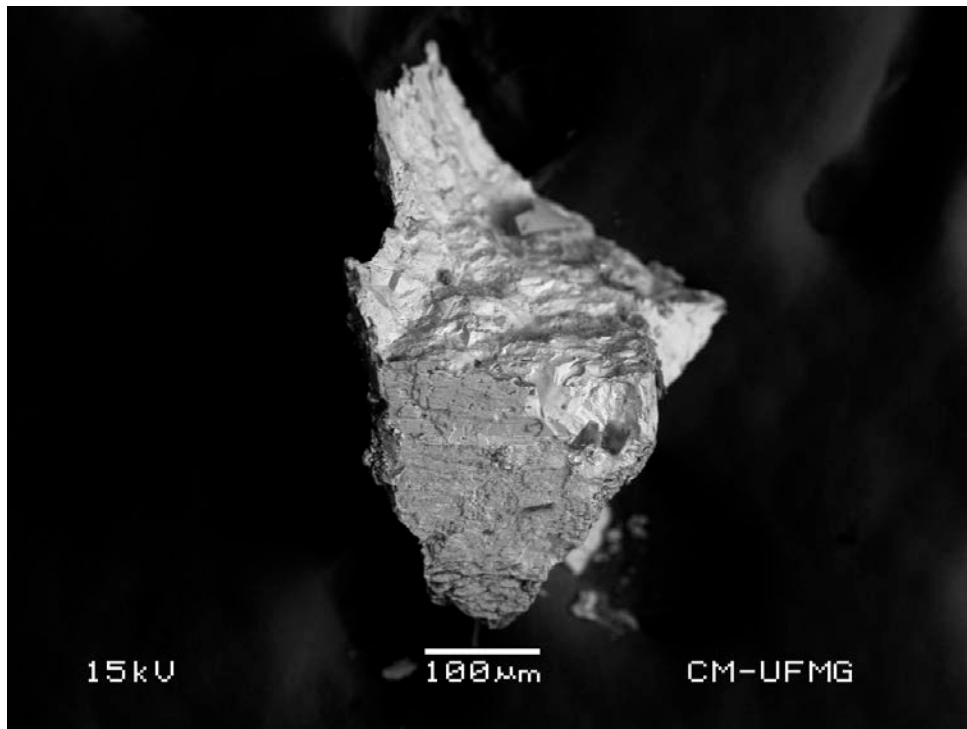
317

318

319

320

321



322

323 **Figure 1 - Backscattered electron image (BSI) of a lulzacite crystal fragment up to 0.5**
324 **mm in length.**

325

326

327

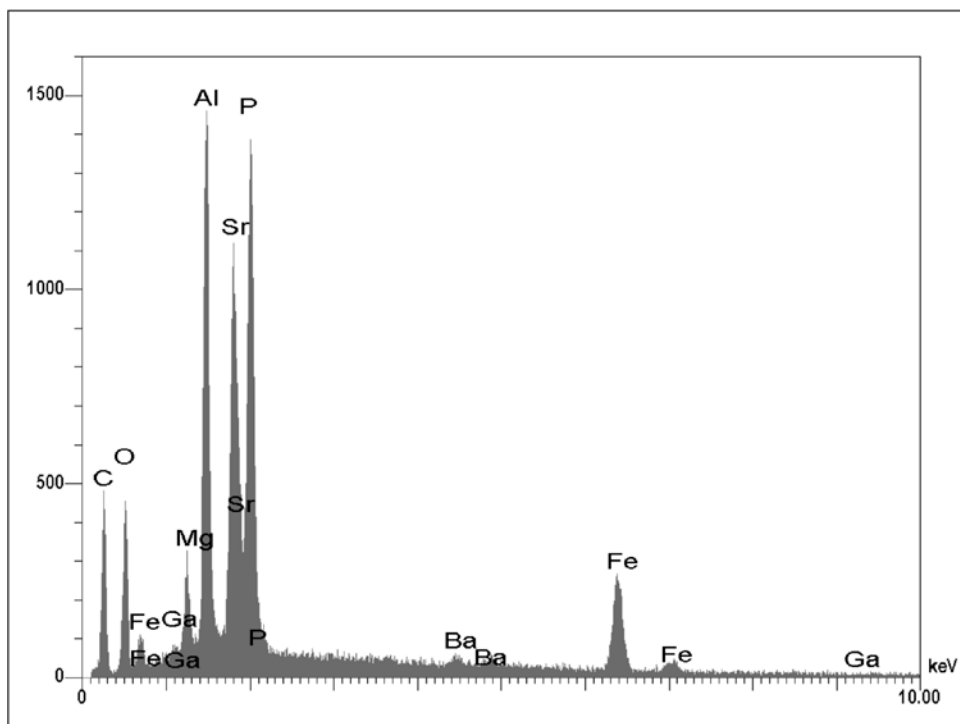
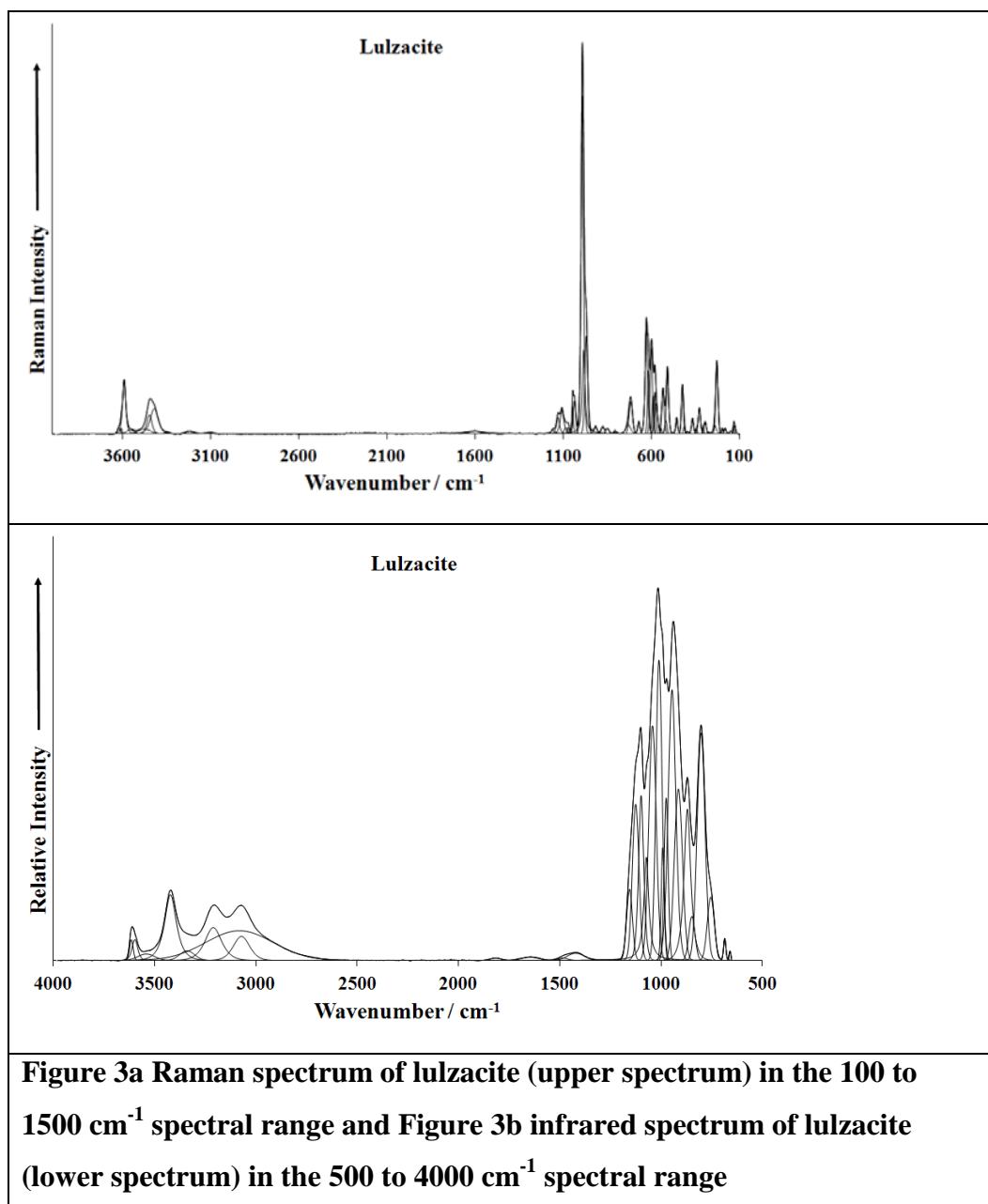


Figure 2 - EDS analysis of lulzacite

332

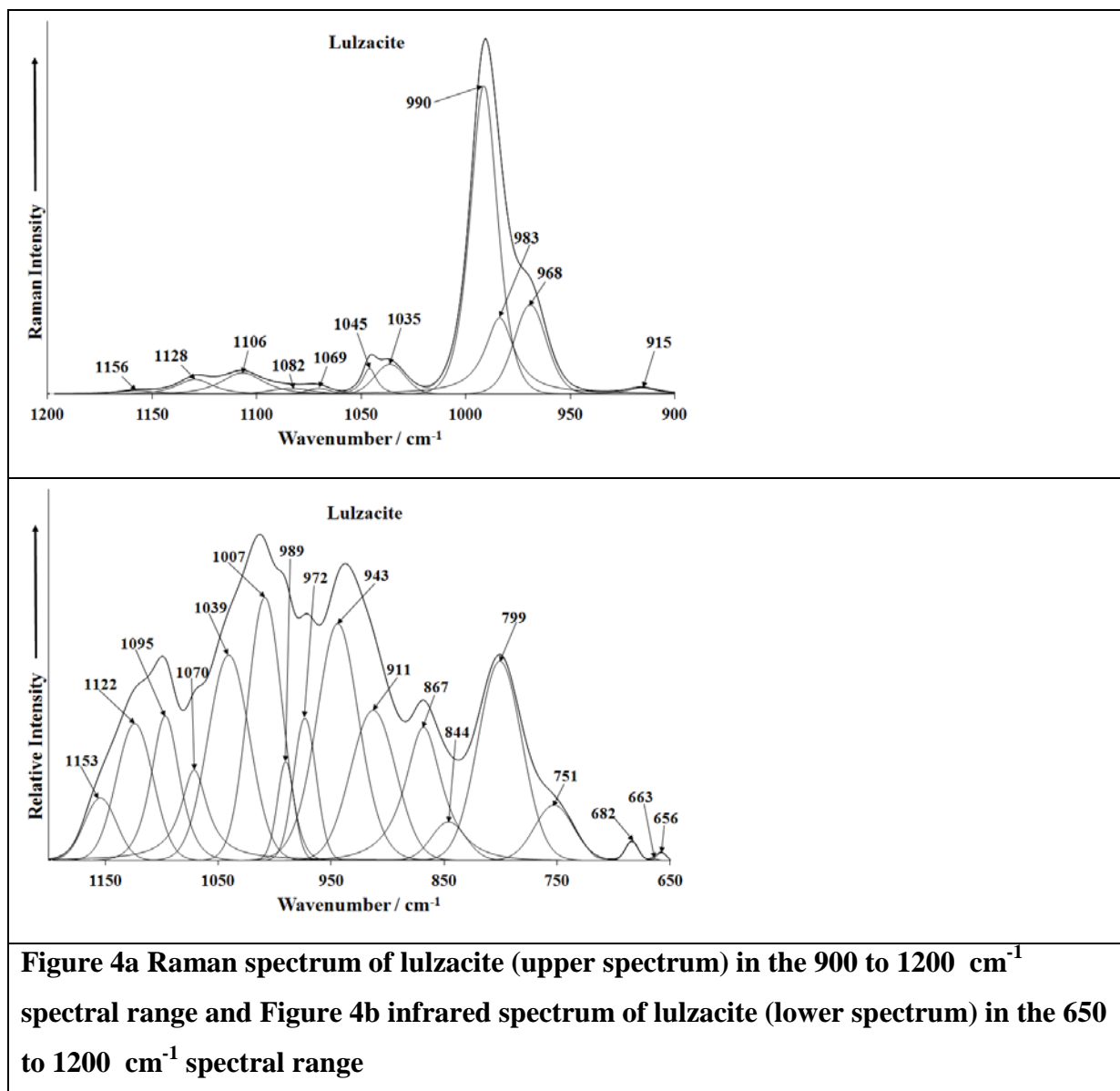
333

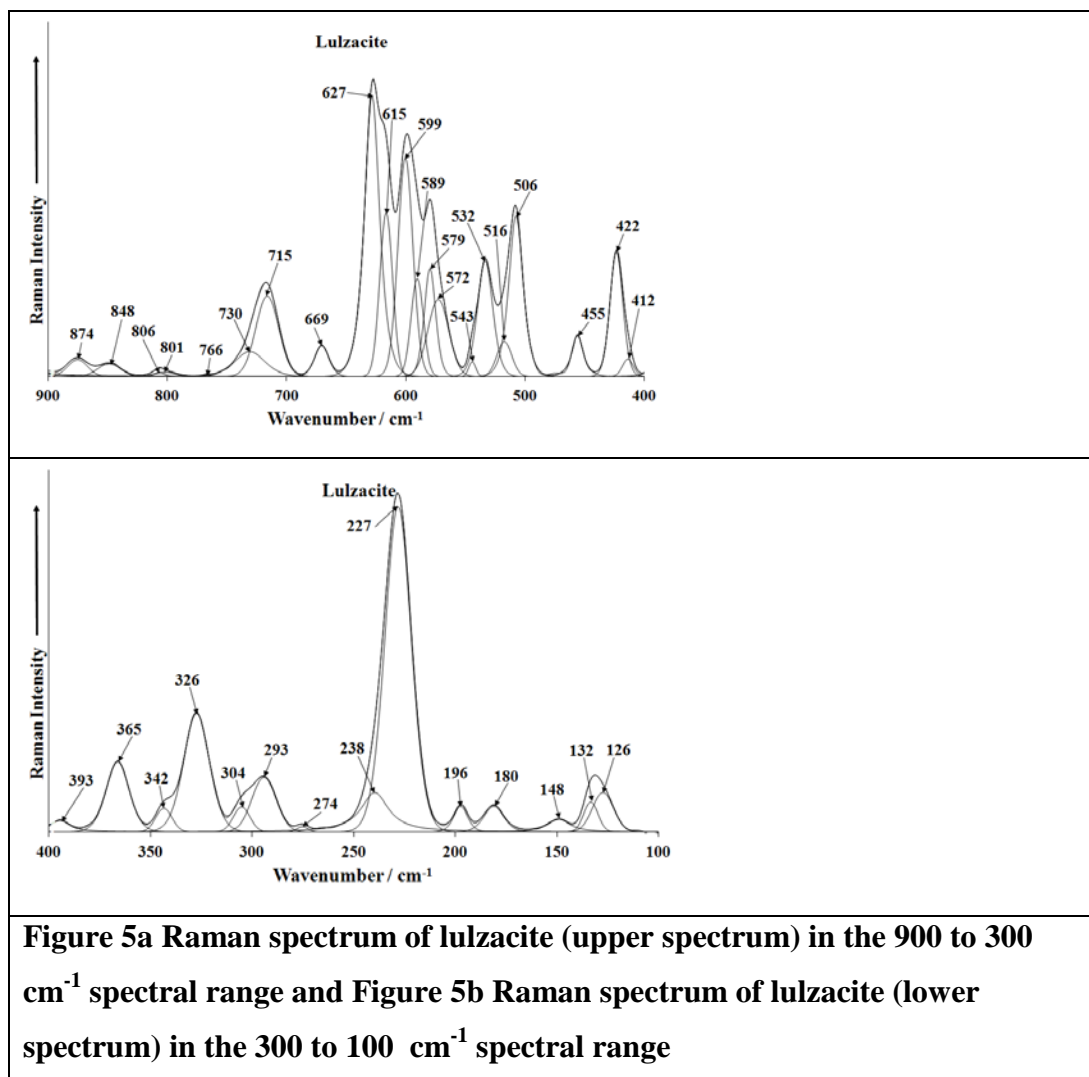


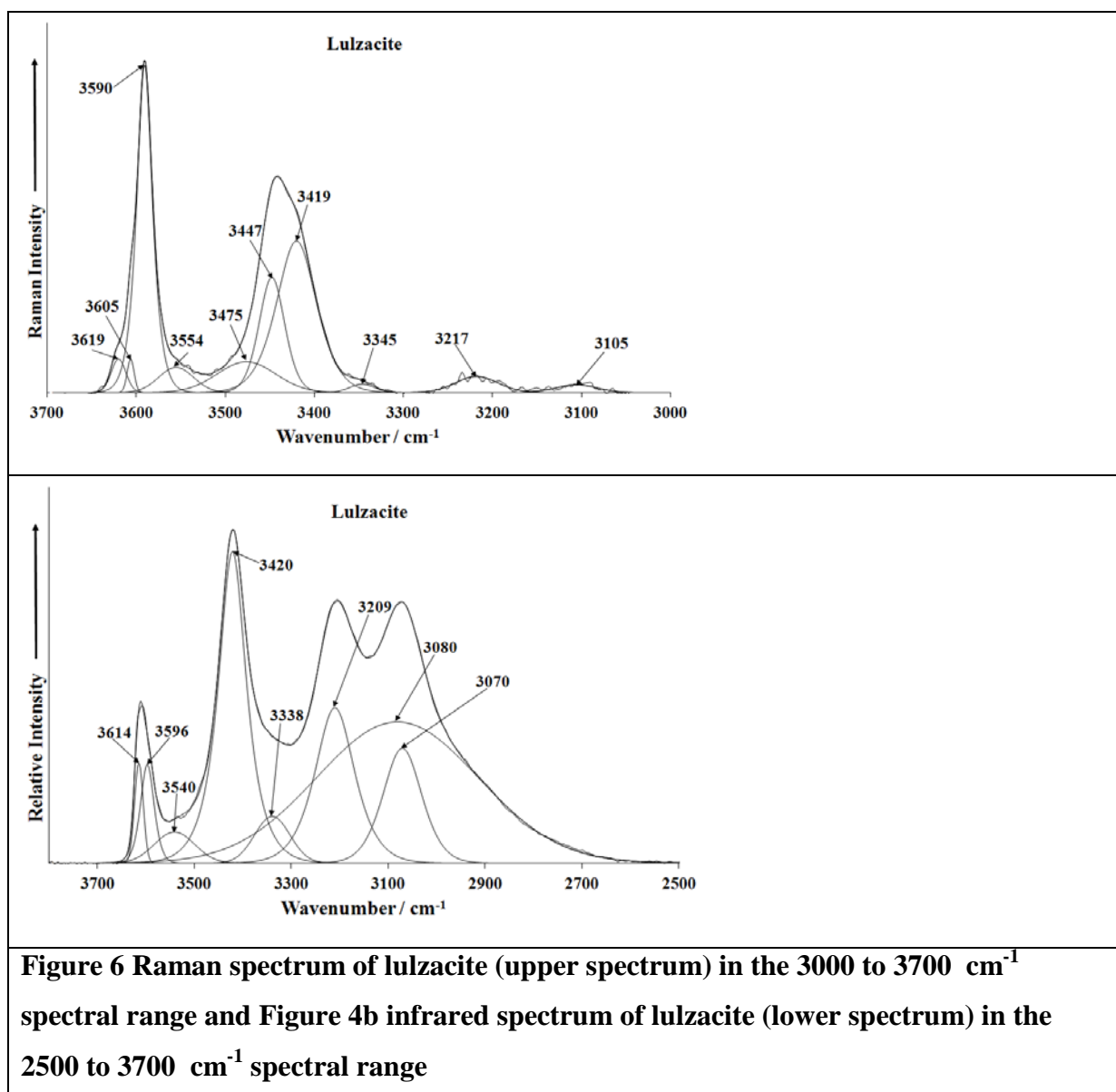
334

335

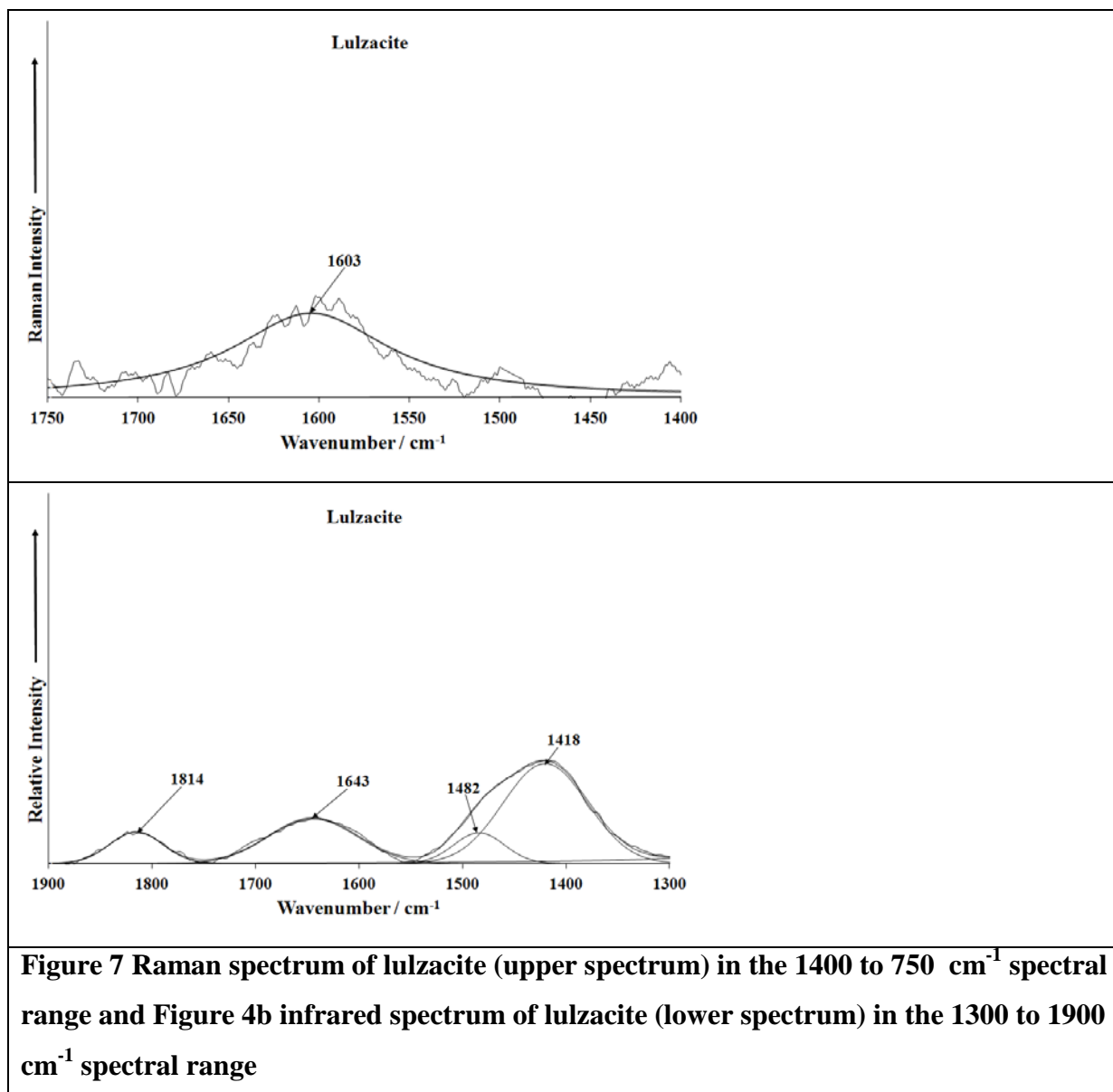
336







343



344

345

346

347